# Anomalous dielectric response in tetrathiafulvalene-*p*-chloranil as observed in temperature- and pressure-induced neutral-to-ionic phase transition

H. Okamoto and T. Mitani
*Institute for Molecular Science, Myodaiji, Okazaki 444, Japan*

Y. Tokura and S. Koshihara
*Department of Physics, University of Tokyo, Tokyo 113, Japan*

T. Komatsu, Y. Iwasa, and T. Koda
*Department of Applied Physics, University of Tokyo, Tokyo 113, Japan*

G. Saito*
*Institute for Solid State Physics, University of Tokyo, Tokyo 106, Japan*
(Received 17 October 1989; revised manuscript received 16 July 1990)

The temperature and pressure dependences of the dielectric constants have been measured on the mixed-stack organic charge-transfer crystal, tetrathiafulvalene-*p*-chloranil, in a frequency range from 100 Hz to 10 MHz. The dielectric response increases remarkably with decreasing temperature down to $T_c = 81$ K, where the neutral-to-ionic (NI) phase transition occurs. On the other hand, with applied pressure at room temperature, the change in the dielectric response is less remarkable, whereas the dc conductivity $\sigma_{dc}$ increases considerably. Such dynamical responses are explained by a Debye-type relaxation model. The strength of the dielectric response is closely correlated with both the relaxation time $\tau$ and $\sigma_{dc}$. These anomalous dielectric responses are attributed to the dynamics of the NI domain-wall pairs and ionic domains in the neutral lattice.

## I. INTRODUCTION

A mixed-stack charge-transfer (CT) crystal, tetrathiafulvalene-*p*-chloranil (TTF-CA) is known to show the so-called "neutral-to-ionic" (NI) phase transition induced by lowering the temperature[1] or by applying pressure.[2] Various measurements have elucidated this unique phase transition.

According to the measurements of infrared molecular vibration spectra,[3,4] the degree of CT ($\rho$) between the TTF donor ($D$) and CA acceptor ($A$) molecules changes sharply from $\sim 0.25-0.3$ to $\sim 0.65-0.7$ at the critical temperature $T_c = 81$K. At the same time, a dimeric distortion of DA stacks occurs at $T_c$.[3-5] Thus, the temperature-induced NI transition is first-order one.

When pressure is applied at room temperature, the DA stacks are also transformed into the dimerized ionic phase at about $P_c = 11$ kbar.[6-8] As the pressure is increased near to $P_c$, dimerized ionic regions are induced within the neutral lattice.[8,9] Such coexistence of the dimerized quasi-ionic regions in the regularly stacked quasineutral regions indicate that both states are almost degenerate in the TTF-CA crystal at high pressures. A similar coexistence of neutral and ionic states has been also observed at ambient pressure when a substitutional impurity such as trichloro-*p*-benzoquinone ($QCl_3$) is doped in TTF-CA crystal.[10]

These features of the NI transition in TTF-CA manifest themselves not only in the optical properties, but also in the electric[11-13] and magnetic[11] properties as a function of temperature and pressure. For instance, the electric conductivity along the stack axis (the **a** axis) shows an exponential dependence upon $T^{-1}$ (except just above $T_c$) with an activation energy of about 0.1 eV both in the neutral ($T > T_c$) and in the ionic ($T < T_c$) region.[11-13] This energy is much smaller than the CT excitation energy of about 0.7 eV.[14,15]

When pressure is applied at room temperature, the conductivity shows an increase by more than 4 orders of magnitude, until it reaches a maximum at about 8 kbar.[9,12] It has been suggested that these characteristic electric properties in the TTF-CA crystal are due to the dynamics of low-energy excitations as charged defects in the form of NI domain walls and solitons.[9,12,13] Here, the NI domain walls are defined as the boundaries between the neutral and ionic domains,[16-18] which are nearly degenerate near the NI phase boundary, while solitons are topological defects in the dimerized one-dimensional DA stacks.[16,18] These charged defects are suggested to become charge carriers because of the fairly small excitation energies.[16,18,19]

The previous optical and electric studies on TTF-CA indicate that the intrinsic charged defects associated with the valence instability of the one-dimensional DA stacks are playing an essential role in the physical properties of TTF-CA near $T_c$ or $P_c$. If this interpretation is valid, the dynamical properties of such charged defects will also manifest themselves as a characteristic dielectric response, as observed in other kinds of one-dimensional incommensurate and commensurate Peierls-Hubbard systems.[20]

 

This paper reports that an anomalous dielectric response has been indeed observed in TTF-CA crystal near $T_c$ and $P_c$. The characteristic behavior of the dielectric constants are closely correlated to the field-dependent dc conductivities which have been recently reported.[13] In contrast to the dielectric responses previously observed in other one-dimensional systems, the dielectric anomaly presently observed in TTF-CA is quite unique, in that the giant dielectric constants and the nonlinear conductivity can be attributed to the valence instability, which is characteristic of the mixed-stack DA complexes near the NI phase boundary. The dynamical behavior of the NI domain wall pairs or the ionic domains within the neutral chains, are inferred from the anomalous dielectric response, as a function of various parameters, such as temperature, field frequency, and pressure.

## II. EXPERIMENTAL

Single crystals of TTF-CA were grown by the cosublimation of the component powder materials which had been purified by conventional recrystallization and sublimation procedures. Thin platelet single crystals, about 0.5 mm thick, were used for electric and dielectric measurements. Silver paste electrodes were painted on both ends of a crystal face.

The real and imaginary parts of the complex ac conductivity $\tilde{\sigma}(\omega)$ were measured in the frequency range of 100 Hz-10 MHz by using an LCR meter (YHP 4274A and 4275A) and an impedance analyzer (YHP 4194A). The former system was employed for the electric measurements using a four-probe configuration at several fixed frequencies, while the latter system was used in two-probe variable-frequencies measurements from 200 Hz to 10 MHz. The amplitude of the applied ac electric field was maintained at values smaller than the threshold for the nonlinear response, which becomes prominent at high fields.[13]

In the measurements at low temperatures, samples were placed in the cold $N_2$ or He gas at atmospheric pressure. In the high-pressure measurements, samples were mounted in a stainless-steel clamp-type high-pressure cell, and hydrostatic pressures were applied through a pressure-transmitting medium composed of a 1:1 mixture of kerosene and diffusion pump oil. The crystal surfaces were coated with an insulating varnish, GE7031, to prevent degradation of the surface in the oil.

## III. EXPERIMENTAL RESULTS

### A. Temperature dependence of dielectric response

The real part $\epsilon_1$ of the dielectric constant $\tilde{\epsilon}$ at ambient pressure was determined from the imagninary part $\sigma_2$ of the complex ac conductivity $\tilde{\sigma}$ by using the relation $\sigma_2(\omega)=j\omega\epsilon_1(\omega)$. The $\epsilon_1$ values were always positive in the experimental range of frequency ($10^2$–$10^7$ Hz) and temperature (2–300 K), over which the measurements were made.

The $\epsilon_1$ values at various frequencies are plotted in Figs. 1(a) and 1(b) as a function of temperature, for the direction of electric field parallel (**E**||**a**) and perpendicular (**E**||**c***) to the stacking axis (the **a** axis), respectively. Note that the dielectric response in the perpendicular direction is nearly 2 orders of magnitude smaller than that in the parallel direction, indicating that the large dielectric constants observed for the **E**||**a** case are certainly due to the dielectric response of the one-dimensional DA stacks.

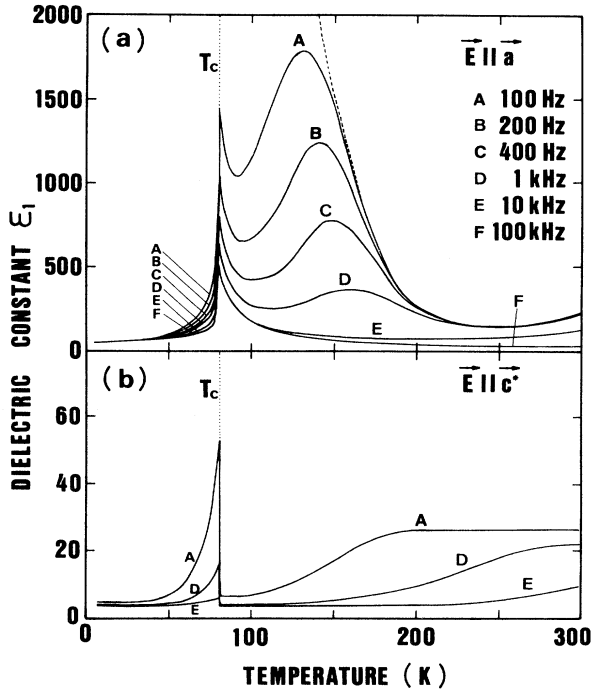


FIG. 1. Temperature dependence of dielectric constant $\epsilon_1$ at several typical frequencies with the electric field parallel to the **a** axis (a) and perpendicular to the **a** axis (parallel to the **c*** axis) (b).

The most significant feature in the results shown in Fig. 1(a) is the remarkable increase of $\epsilon_1$ in the neutral phase above $T_c$, while the $\epsilon_1$ shows only a slight temperature dependence in the ionic phase below $T_c$. For instance, the $\epsilon_1$ value at room temperature is about 250 at 100 Hz. When temperature is lowered, the $\epsilon_1$ value decreases slightly, until a minimum is reached at around 230 K, and then shows a remarkable increase at lower temperatures toward a maximum of about 1800 at about 130 K. After passing this maximum, the $\epsilon_1$ value decreases again until it sharply increases near $T_c$, showing a divergent behavior at $T_c$. The temperature dependence of $\epsilon_1$ at low frequencies is thus characterized by a broad maximum at a temperature somewhere between room temperature (RT) and $T_c$, followed by a steep, divergent, peak at $T_c$. It is shown that in the following discussion, such a broad peak is actually a superficial effect due to the temperature dependence of the relaxation frequency in the dielectric response.

At higher frequencies, the dispersive behavior of $\epsilon_1$ above $T_c$ becomes less prominent, and at frequencies

higher than 10 kHz, there is no steep increase of $\epsilon_1$ below 200 K, except for a trace of divergentlike increase near $T_c$.

The frequency dependences of the real and imaginary parts of the dielectric constant ($\epsilon=\epsilon_1-j\epsilon_2$) for the E||a geometry are plotted in Fig. 2 for three fixed temperatures, which are somewhat arbitrarily chosen at 297, 234, and 188 K, all in the neutral phase above $T_c$. The experimental values for $\epsilon_1$ and $\epsilon_2$ shown in Fig. 2 were determined by assuming an equivalent circuit composed of a parallel resistance $R$ and a dielectric substance having the complex dielectric constant $\tilde{\epsilon}$, as shown in the inset in Fig. 2. The $\tilde{\epsilon}$ was derived from $\tilde{\sigma}$ by using the following equations: $\epsilon_1=\sigma_2/(\epsilon_0\omega)$, $\epsilon_2=(\sigma_1-\sigma_{dc})/(\epsilon_0\omega)$, $\sigma_{dc}=d/(RS)$. Here, $S$ and $d$ are the cross section and the thickness of the sample, respectively. (We note that the absolute magnitudes of $\epsilon_1$ are different between the results shown in Figs. 1 and 2. For an example, the low-frequency value of $\epsilon_1$ at room temperature is about 250 in the results shown in Fig. 1, whereas it is a little larger than 500 in the results shown in Fig. 2. These differences are partly due to the approximation in the data analysis of the respective measurements and also perhaps partly due to sample-to-sample variation.) According to a simple Debye-type relaxation model,[21] the real and imaginary parts of dielectric function are expressed by

$$\epsilon_1(\omega)=\epsilon_\infty+\frac{\epsilon(0)-\epsilon_\infty}{1+\omega^2\tau^2} \tag{1a}$$

and

$$\epsilon_2(\omega)=\frac{\epsilon(0)-\epsilon_\infty}{1+\omega^2\tau^2}\omega\tau\ . \tag{1b}$$

Here, $\epsilon(0)$ and $\epsilon_\infty$ are static and high-frequency dielectric constants, respectively, and $\tau$ is the relaxation time. The characteristic frequency $f=(2\pi\tau)^{-1}$ corresponds to the maximum of the $\epsilon_2$ curve. The experimental $\epsilon_{1,2}$ curves shown in Fig. 2 can be fitted to the Debye model fairly well. From the maxima of $\epsilon_2(\omega)$ curves at various temperatures we could determine the experimental values for $f$ at respective temperatures. The results are shown by solid circles in a semilogarithmic plot against $T^{-1}$ in Fig. 3. In the same figure we have also plotted the temperature dependence of dc conductivity $\sigma_{dc}$ (open circles), in a scale normalized to the value at room temperature ($\sigma_{RT}$). The lines are nearly parallel to each other, both having the activation energy of about 0.08 eV. The similarity between the temperature dependences of $f$ and $\sigma_{dc}$ will be discussed later in Sec. IV.

Because of experimental limitations we could not make reliable measurements of the $\epsilon_{1,2}(\omega)$ curves at temperatures below about 150 K. However, the results shown in Fig. 3 can explain why the $\epsilon_1$ curves in Fig. 1, as a function of temperature, show a broad maximum somewhere between RT and $T_c$. As the temperature is lowered below 250 K, the $\epsilon_1$ values for frequencies below 400 Hz increase, being weakly dependent on frequency. This is attributed to a monotonous increase of $\epsilon(0)$, as the temperature is lowered. But, at the same time, the characteristic frequency $f$ decreases (as seen in Fig. 3), causing a reduction of $\epsilon_1$ at frequencies higher than $f$. This explains the observed feature of $\epsilon_1$ curves (broad maximum between $RT$ and $T_c$) shown in Fig. 1(a). According to this interpretation, the temperature dependence predicted for $\epsilon(0)$ should be dramatic: the hypothetical $\epsilon(0)$ curve is shown in Fig. 1(a) by a dotted line. At about 100 K, it will attain a value of the order of $10^4$ for the E||a geometry. On the other hand, the divergent increase of $\epsilon_1$ observed just above $T_c$ is almost independent of frequency [Fig. 1(a)], indicating a second contribution, from a higher-frequency response, which increases in approaching to $T_c$.

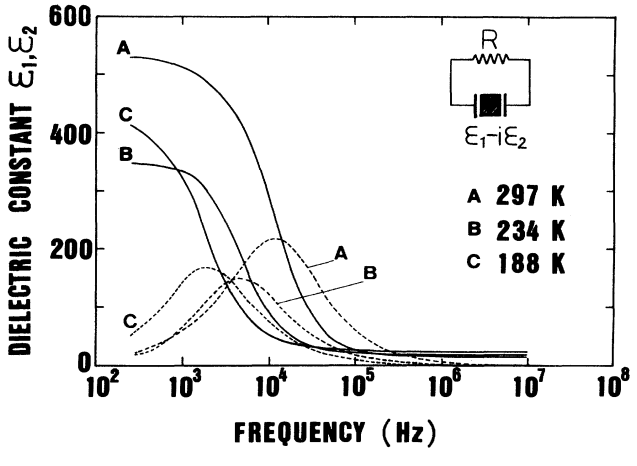


FIG. 2. Frequency dependence of dielectric constants $\epsilon_1$ (solid lines) and $\epsilon_2$ (broken lines) along the **a** at 297 K (A), 234 K (B), and 188 K (C). The equivalent circuit composed of the resistance and the dielectric substance is shown in the inset.

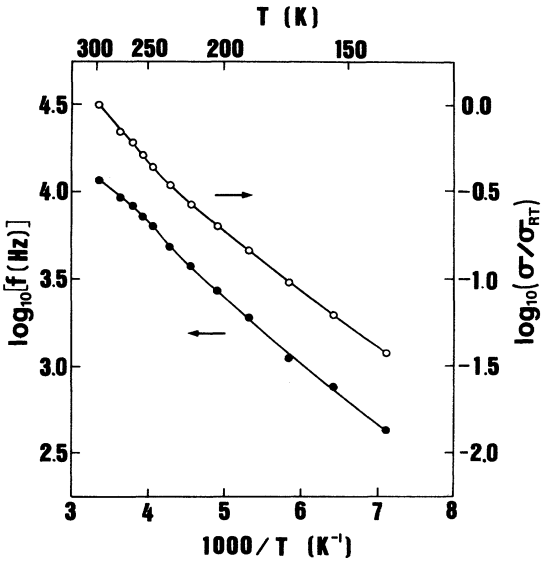


FIG. 3. Temperature dependences of the relaxation frequency $f$ and the dc conductivity $\sigma$. The conductivity is normalized by the value $\sigma_{RT}$ at room temperature.

### B. Pressure dependence of the dielectric response

The dielectric constants, $\epsilon_1$ and $\epsilon_2$, observed at room temperature under various pressures are plotted in Fig. 4, as a function of frequency. The features of the $\epsilon_{1,2}$ curves can be again explained by a Debye-type relaxation model. The saturation values of $\epsilon_1$ at low frequencies change slowly up to 3.5 kbar. On the other hand, the peak in the $\epsilon_2$ curve shifts to higher frequency, indicating an increase of the relaxation frequency $f$ with pressure. The values for $f$ are plotted against pressure in Fig. 5 (solid circles). At pressures of about 4 kbar, the $f$ value becomes as large as about $10^7$ Hz. In the same figure we also plotted the pressure-dependence of dc conductivity $\sigma$ (open circles), normalized to the $\sigma$ value ($\sigma_{AP}$) under atmospheric pressure and at room temperature. The $\log_{10}(f)$ and $\log_{10}(\sigma/\sigma_{AP})$ curves are both linear with pressure, with almost the same slopes. From Figs. 3 and 5 we suggest that the current carriers responsible for both the dc conductivity and the Debye-type dielectric response under an ac electric field are identical in origin. More detailed discussion on this point will be given in the next section.

From previous optical[8,9] studies of the pressure effect in TTF-CA, it has been concluded that a part of neutral stacks is converted to dimerized ionic regions by the application of pressure. The density of ionic molecules increases with pressure, until the whole lattice is converted to the ionic phase at about 11 kbar.[8,9] In accord with this there occurs a change in the dielectric response when pressure becomes higher than about 4 kbar. In Fig. 6 we plot the pressure dependence of $\epsilon_1$ at various frequencies up to about 7 kbar.[22] A significant point in this plot is that the $\epsilon_1$ values at low frequencies decrease with pressure, and finally become negative at high pressures. Such a feature is not seen in the low-pressure behavior ($p < 3.5$ kbar) of $\epsilon_1$ shown in Fig. 4, but when pressure exceeds about 4 kbar, it turns out that the $\epsilon_1$ value becomes negative at low frequencies. The crossing point $f_c$, where $\epsilon_1$ becomes zero, is located at about 10 kHz at around 5 kbar, and the $f_c$ shifts to higher frequencies with increasing pressure. Such a frequency dependence of $\epsilon_1$ can no longer be dealt with by a Debye-type model. This dielectric anomaly at $f_c$ implies that some kind of self-oscillation mode is excited at this frequency when pressure exceeds about 4 kbar. An interpretation of this effect will be given in the next section.

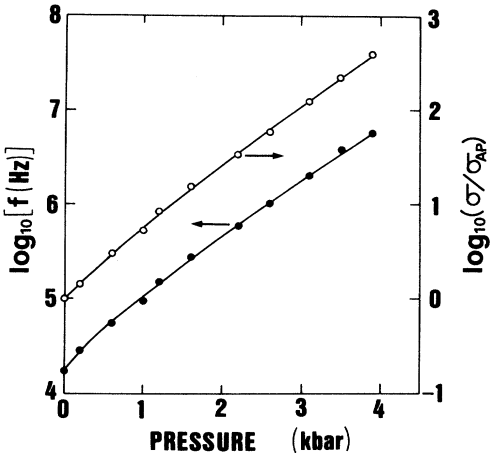


FIG. 5. Pressure dependences of the relaxation frequency $f$ and the dc conductivity $\sigma$ at room temperature. The conductivity is normalized by the value $\sigma_{AP}$ at ambient pressure.

## IV. DISCUSSION

### A. The dynamics of NI domain walls: A qualitative model of dielectric response and dc conductivity

Before going to detail discussions on the experimental results presented in the preceding section, it would be in-

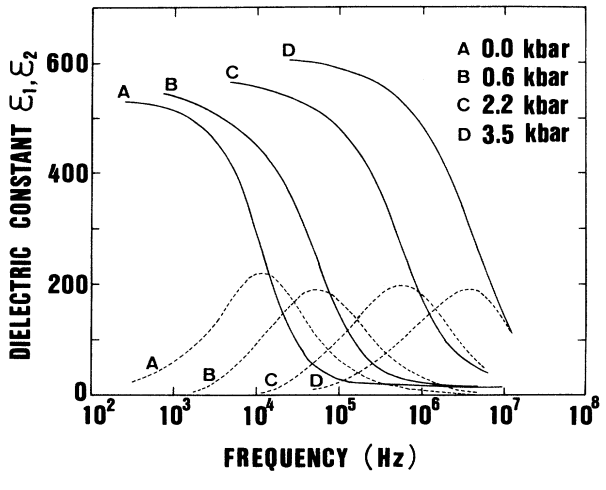


FIG. 4. Frequency dependence of dielectric constants $\epsilon_1$ (solid lines) and $\epsilon_2$ (broken lines) along the **a** axis at 0.0 kbar (A), 0.6 kbar (B), 2.2 kbar (C), and 3.5 kbar (D).

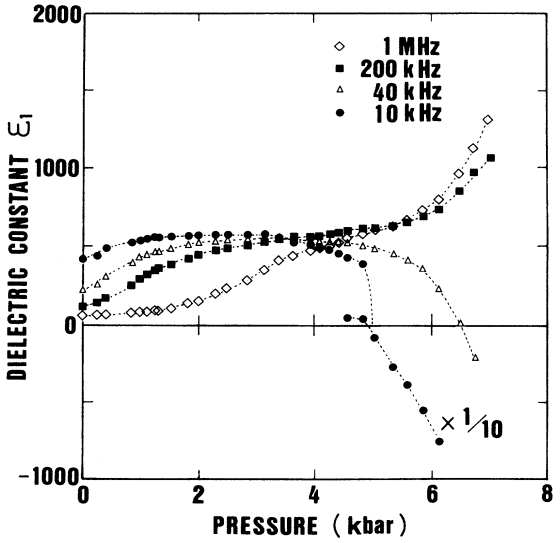


FIG. 6. Pressure dependence of dielectric constant $\epsilon_1$ along the **a** axis at several typical frequencies of the applied field.

structive to summarize here the qualitative aspects of dielectric response and dc conductivity in TTF-CA crystal. A picture of NI domain walls (or equivalently the ionic domains excited in the neutral lattice) has been previously proposed to explain the optical properties under hydrostatic pressure[6,8,9] and in the doped crystal.[10] The mechanism of dc transport has been also discussed in terms of such NI domain walls.[9,12,13,18] It is quite likely, as mentioned before, that the same microscopic mechanism is responsible for the dc conductivity and the dielectric response, if we consider the remarkable similarity discovered between the relaxation frequency and the dc conductivity as a function of temperature (Fig. 3) or pressure (Fig. 5). We propose as a model for the dielectric response, a picture of NI domain walls.

Let us consider an ionic domain which is induced in a neutral stack, as schematically illustrated in Figs. 7(b) and 7(c). Such an ionic domain will contain a certain number of dimerized $D^+A^-$ pairs as a cluster, since an energy is gained as the electrostatic Madelung energy between the ionic molecules in favor of the clustering of $D^+A^-$ pairs. However, the energy (per molecule) of the ionic region must be still higher than that of the neutral region at temperatures above $T_c$, so that the ionic domain will be confined within a finite size, as shown in Figs. 7(b) and 7(c). Such an ionic domain can be regarded as an NI domain wall pair, which is analogous to a bipolaron in nondegenerate conjugated polymers like cis-polyacetylene. However, in the case of mixed-stack *CT* crystals (analogous to an *AB* polymer), there are two equivalent configurations in ionic domains, as depicted by *IA* and *IB* in Figs. 7(b) and 7(c). Both of these domains have finite dipole moments, which are directed in opposite directions. When an electric field is applied along the stack axis, the energies for these domains are slightly changed, depending on the direction of dipole moment. As a result, the sizes and/or the relative numbers of *IA* and *IB* domains will be modified differently by the electric field. At thermal equilibrium in an electric field, a finite nonzero electric polarization is induced in this way in the crystal.


FIG. 7. Schematic structures of donor($D$)-acceptor($A$) chain: (a) neutral chain, (b) neutral-ionic domain wall (*NIDW*) pair (domain *IA*), (c) *NIDW* pair (domain *IB*), (d) ionic chain (*IA*), (e) spin-soliton pair, (f) ionic chain (*IB*), (g) *NIDW* pair, (h) polaron pair, (i) charged-soliton pair. $\rho_{NIDW}$, $\rho_{SS}$, $\rho_P$, and $\rho_{CS}$ are effective charges of *NIDW*, spin soliton, polaron, and charged soliton, respectively. Arrows show the direction of dipole moments.

We proceed to the discussion about the dc transport mechanism based upon the NI domain walls. When an external electric field is applied along the stack axis, say to the left, in Fig. 7(b), the domain *IA* is enlarged. The energy needed for enlarging its size to infinity corresponds to the binding energy of an NI domain wall pair. This process induces only a displacement current in the chain and a stationary current flow cannot be supported by such a process alone. In order to explain the stationary dc conductivity in TTF-CA crystal, a model has been proposed by Nagaosa in terms of solitons and NI domain walls.[18] This model is summarized as follows. For a dc transport to occur after the processes $(a)\rightarrow(b)\rightarrow(d)$ in Fig. 7, the resulting dimerized ionic chain *IA* [Fig. 7(d)] should be converted again to *IB* [Fig. 7(f)]. This is achieved by the process of excitation and dissociation of a spin-soliton pair as shown in Fig. 7(e). Note that these spin solitons in a donor-acceptor crystal have fractional charges which can be driven to opposite motions by the field. The final process is the conversion of the ionic state *IB* [Fig. 7(f)] to the neutral state [Fig. 7(a)] by the excitation and dissociation of an NI domain wall pair, as shown in Fig. 7(g). Effective charges of the NI domain walls and solitons are denoted in Fig. 7 as $\rho_{NIDW}$ and $\rho_{SS}$. In this model, the polaronlike ionic domains [Fig. 7(h)] can be regarded as the current carriers in the neutral phase. They are produced by the dissociation of the ionic domains [Figs. 7(b) and 7(c)]. We note that, in the limit where the size of such a polaron tends to become sufficiently large, the polaron excitation is equivalent to the simultaneous excitations of an NI domain-wall pair and a spin-soliton.

### B. Temperature dependence of $\bar{\epsilon}$

In the following we present the phenomenological model to interpret the temperature dependence of $\bar{\epsilon}$ in detail based upon the above-mentioned NI domain wall mechanism. In the case of the equivalent circuit composed of a parallel resistance and a dielectric substance as shown in Fig. 2, the time-dependent current density $j(t)$ after the sudden application of a field $E$ is described as follows:[23,24]

$$j(t)=\sigma_0 E\exp(-t/\tau)+\sigma_{\rm dc}E\ . \tag{2}$$

The first and second terms represent the transient and stationary current, respectively. The strength of the

dielectric response $[\epsilon(0)-\epsilon_\infty]$ is given by the following relation:[23,24]

$$\epsilon(0)-\epsilon_\infty=(\sigma_0/\epsilon_0)\tau\ , \tag{3}$$

where $\epsilon_0$ is the permittivity of free space. The experimental values of $[\epsilon(0)-\epsilon_\infty]$, $\tau$, and $\sigma_{dc}$ for TTF-CA at ambient pressure can be evaluated from the results presented in Figs. 2 and 3. In Fig. 8 we plot the experimental values of $[\epsilon(0)-\epsilon_\infty]$, obtained from the results shown in Fig. 2 (Ref. 25) and Fig. 3, as a function of temperature (solid squares). In the same figure we also plot the experimental values for $(\sigma_{dc}/\epsilon_0)\tau$, which is the quantity corresponding to the right side of Eq. (3) with $\sigma_0$ replaced by $\sigma_{dc}$ (solid triangles). Note that temperature dependences of these two quantities are almost parallel to each other. This implies that $\sigma_0$ is proportional to $\sigma_{dc}$ in TTF-CA in the temperature range of Fig. 8. In this model we can assume that pairs of effective charges are located at the NI domain walls. The conductivities $\sigma_0$ and $\sigma_{dc}$ are attributed to the contributions of bound and unbound charge associated with the NI domain walls.

In the present model, the dielectric response is determined by two factors; the nonequal numbers of the domains *IA* and *IB*, and the field-induced change in the domain size. In the following we assume that the field-induced change in the number of the domains *IA* and *IB* is negligible (as proved to be the case later) and that only the change in size of the ionic domains induced by the electric field is playing the dominant role. Let us consider an ionic domain which contributes to the dielectric response. It must be confined in a region of finite size, so that we may simulate the dielectric response of it by the stretching oscillation of an electric dipole moment within a harmonic potential, as schematically illustrated in Fig. 9. Here, $p_0$ is the equilibrium dipole moment of the domain in the absence of external electric field. For the present system, which is well described by an overdamped oscillator model, the relaxation time $\tau$ is given by $(\tau_0\omega_0^2)^{-1}$,[26] where $\omega_0^2$ corresponds to the restoring force

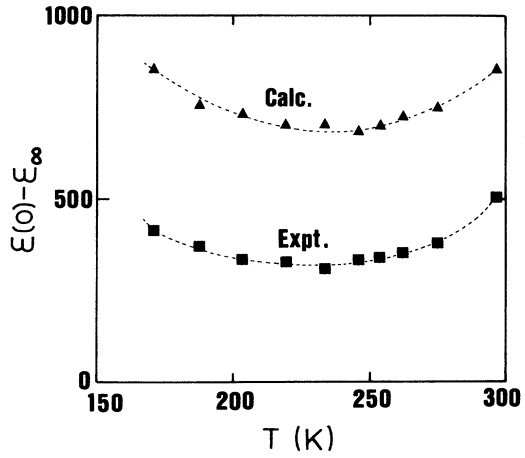


FIG. 8. Temperature dependence of $[\epsilon(0)-\epsilon_\infty]$, squares for experimental values, and triangles for calculated $\sigma_{dc}\tau/\epsilon_0$ values.

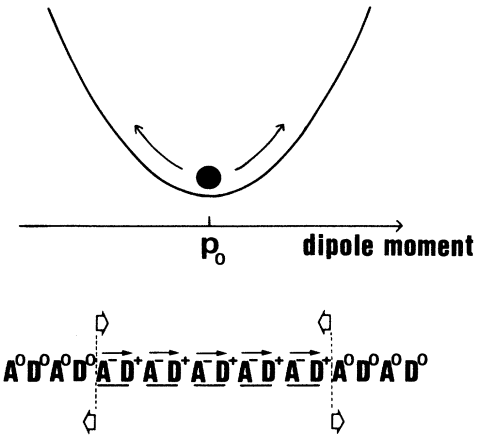


FIG. 9. Schematic illustration of stretching oscillation of a confined ionic domain moving in a harmonic potential. $p_0$ is the dipole moment of the ionic domain in the absence of external electric field.

and $\tau_0^{-1}$ to the damping coefficient. The latter is related to the intrinsic mobility $\mu$ by the following general formula:

$$\mu=\rho_0\tau_0/m^*\ . \tag{4}$$

Here, $\rho_0$ and $m^*$ represent the effective charge and the effective mass of an *NIDW*. Substituting Eq. (4) to Eq. (3) and using the relation $\tau=(\tau_0\omega_0^2)^{-1}$, we get an expression for the strength of the dielectric response as follows:

$$\epsilon(0)-\epsilon_\infty=K(\sigma_0/\omega_0^2\mu)\ . \tag{5}$$

Here, the temperature-independent prefactor $K$ is defined as $K=\rho_0/\epsilon_0 m^*$. The temperature variation of the left side of Eq. (5) is ascribed, in the present model, to the temperature-dependent parameters $\sigma_0$, $\omega_0^2$, and $\mu$. The temperature dependence of the left side of Eq. (5), $[\epsilon(0)-\epsilon_\infty]$, is experimentally known and is plotted in Fig. 8. It is utterly different from that of $\sigma_{dc}$ (Fig. 3), which is proportional to $\sigma_0$. These results are understandable if we assume that the temperature dependences of $\sigma_{dc}$ and $\tau^{-1}$ are mainly determined by the temperature-dependent mobility $\mu$, which is a sole common factor in both parameters, $\sigma_{dc}(=n\rho_0\mu)$ and $\tau^{-1}(=m^*\mu\omega_0^2/\rho_0)$. This implies at the same time that the carrier density $n$, that is, the number of the NI domain walls, must be less temperature dependent than the mobility $\mu$.

In TTF-CA, the bound and unbound charges on NI domain walls, responsible for the dielectric response and dc conductivity, are strongly coupled to the lattice by the effect of the electron-lattice interaction, so that there is a finite barrier for the motion of charged carriers. It is the reason why the mobility $\mu$ is determined by the thermal activation-type formula.

Here, based on the arguments mentioned above, we speculate the mechanism of thermal behaviors of static dielectric constant as follows. Since the quantity $\sigma_0/\mu$ is nearly temperature independent, the temperature varia-

tion of the static dielectric constant should be predominantly determined, according to Eq. (5), by the temperature dependence of $\omega_0^{-1}$. This is quite understandable for TTF-CA. When temperature is lowered to $T_c$, the energy of the ionic state will be lowered with respect to the energy of the neutral state, leading to an increase of the size of confined ionic domains. This causes a decrease of the restoring force $\omega_0^2$ for the motion of the NI domain wall pair.

In the above discussion we have assumed that the relative number of the oppositely polarized domains $IA$ and $IB$ are not influenced significantly by the electric field. Otherwise, we shall have to consider the bulk polarization induced by the unequal numbers of $IA$ and $IB$ existing in the thermal equilibrium under the electric field. If this is the case, $[\epsilon(0)-\epsilon_\infty]$ would contain a term which is temperature dependent in proportion to $np_0^2/kT$. However, we could not discriminate experimentaly such an effect, if any, in the observed electric response. In this sense, the above model for the dielectric response, which is essentially based on the field-induced change in the domain size, is reasonably consistent with the existing experimental results.

In the temperature dependences of $\epsilon_1$ shown in Fig. 1(a) we have noticed that the $\epsilon_1$ values show a sharp increase in a narrow temperature region just above $T_c$. Such a steep increase of $\epsilon_1$ near $T_c$ seems to be essentially independent of frequency in the measured frequency region. This fast component is likely to be a manifestation of a first-order-like transtion of TTF-CA crystal to an antiferroelectrically ordered phase of dimerized $DA$ stacks at $T_c$.

Now, we turn our attention to the possible relation between the dielectric response and the nonlinear dc conductivity which has been recently found in both neutral and ionic phases.[13] The most remarkable feature of this nonlinearity is the strong enhancement of it as temperature is lowered to $T_c$. This behavior has been interpreted as follows. The dc conductivity in the neutral phase is supported by the dissociation process of NI domain wall pairs, which is enhanced by an external electric field. Such an enhancement of the dissociation process occurs more easily as the temperature approaches $T_c$. In this temperature region, where the nonlinearity of $\sigma_{dc}$ becomes remarkable, the $\epsilon_1$ values also show a considerable nonlinear dependence on the electric field. It has been observed that the $\epsilon_1$ values are decreased when the amplitude of an applied ac electric field exceeds a threshold value for the nonlinear conductivity.[27] This result is consistent with the interpretation that the bound NI domain wall pairs responsible for the dielectric response at low fields are dissociated by a strong electric field, and contribute to the nonlinear conductivity at high fields.

In the preceding discussions we were mainly concerned with discussion on the anomalous dielectric response observed in the neutral phase near $T_c$. As for the dielectric response in the ionic phase ($T < T_c$), it has been noticed that the relaxation frequency $f$ is appreciably decreased with decreasing temperature. The $f$ value becomes smaller than the lowest observable limit frequency (about 100 Hz) in the measurement shown in Fig. 2. In this temperature region, spin solitons or charged solitons [Figs. 7(e) and 7(i)] are suggested to be the dominant charge carriers for electric conductivity. The dynamics of these solitons are supposed to play an important role in the dielectric response, too.

### C. Pressure dependence of $\tilde{\epsilon}$

We proceed to discussion on the dielectric response under high pressures. In the relatively low-pressure region (up to about 4 kbar), the effect of pressure on the dielectric response is qualitatively similar to what we have observed when temperature is lowered at ambient pressure (compare the results shown in Figs. 2 and 4). The dc conductivity and the relaxation frequency are both increased with pressure, as shown in Fig. 5. These results will be likewise ascribed to the increase of the mobility $\mu$ with pressure. From the plot in Fig. 6 it is seen that the dielectric constant at low frequencies does not change so much by pressure, until it reaches a critical value of about 5 kbar. The $\{\epsilon(0)-\epsilon_\infty\}$ values can be estimated in this pressure region by substituting the experimental $\sigma_{dc}$ values for $\sigma_0$ in Eq. (3). These values were found to be almost constant, so that the arguments made before for the temperature dependence of the dielectric response, seems to be also valid for the pressure-dependence in this pressure range.

When pressure is raised further, beyond a critical value $P_0 \doteqdot 5$ kbar, the low-frequency dielectric constant exhibits an abrupt drop to zero, and then it becomes negative at pressures higher than $P_0$ as seen in Fig. 6. We suggest the following interpretation for the negative $\epsilon_1$ values above $P_0$. As the energies of the ionic and neutral states become nearly degenerate with pressure, the restoring force for the motion of an NI domain wall pair will be diminished, and finally vanish at around $P_c$. It may happen, then, that the effective charges of individual molecules are quickly fluctuating between the mixed-valent bistable states, corresponding to those of the ionic state [Figs. 7(d) or 7(f)] and the neutral state [Fig. 7(a)] under the influence of a low-frequency ac electric field. Because of the long-range electrostatic interaction between these charged molecules, the fluctuating charge-transfer processes in the individual $DA$ pairs will be correlated to each other, and form a collective oscillation, that is, a plasmonlike oscillation under the electric field. According to this interpretation, the frequency $f_c$, at which $\epsilon_1$ becomes zero at a fixed pressure, corresponds to the plasma frequency. The $f_c$ is located at about 10 kHz at around 5 kbar, and increases with pressure to about 40 kHz at 6.5 kbar. In the damped oscillator model presently employed, such an increase of $f_c$ can be explained by a decrease of the damping coefficient $\tau_0^{-1}$ with pressure.

Thus, under high pressures and at room temperatue, the NI domain wall pairs [Fig. 7(g)] or the ionic domains in the neutral lattice [Figs. 7(b) and 7(c)] become more loosely bound, and tend to behave as unbound charge carriers. The contribution of these carriers is larger in the pressure-induced dc conductivity[9,12] than in the pres-

sure dependence of dielectric response. (Such a situation is similar to the case where a strong electric field is applied at low temperatures.) At the same time, it has been observed that the nonlinearity in dc conductivity becomes less prominent as pressure is increased.[28] This result is also consistent with the present interpretation.

It is interesting here to consider why the dielectric response is different for the temperature-induced NI transition (TINIT) than for the pressure-induced NI transition (PINIT). We note that, in the case of TINIT, the NI phase transition is mainly driven by a combined effect of the energy gain by the lattice dimerization, due to the electron (spin)-lattice interaction, and by the Madelung energy. On the other hand, in the case of PINIT, the effect of Madelung energy is supposed to play a dominant role.[29] The ionic regions induced in the neutral lattice by pressure are dimerized, as seen by the IR measurements.[6,8] However, at room temperature, the effect of the electron-lattice interaction is still relatively small, so that the dimeric molecular displacement in the pressure-induced ionic region is not stable, but is thought to be fluctuating in both time and space, in contrast to the static dimerization at low temperatures, as supported by several experimental results.[8,9] We speculate that, at room temperature, the collective (plasmonlike) response of the $DA$ pairs occurs more easily under pressure. Another important point is that the pressure-induced NI transition occurs more continuously, as compared to the temperature-induced NI transition, while both the NI transitions are essentially first order. In the PINIT, the restoring force of an NI domain wall pair is reduced to zero at high pressures, whereas it remains finite in the TINIT even as the temperature is lowered to just above $T_c$. In short, free motion of charged NI domain walls is possible only in the PINIT case and the dielectric response does exhibit a plasmonlike behavior at high pressures, but it does not at low temperatures.

## V. CONCLUSION

An anomalous dielectric response has been observed in TTF-CA crystal at low temperatures and at high pressures, where the lattice undergoes the NI transition. From the analysis of experimental results, it has been shown that the observed dielectric response in the neutral phase is consistently accounted for by the dynamics of the NI domain wall pairs and the ionic domains embedded in the neutral lattice.

There is a significant difference between the effects of temperature and pressure on the dielectric response. A remarkable increase of the dielectric constant is observed when temperature is lowered to $T_c$, whereas the dc conductivity decreases monotonically, following an exponential dependence on $T^{-1}$. On the other hand, when pressure is applied at room temperature, the dielectric constant is nearly pressure independent in the low-pressure region, whereas the dc conductivity is considerably increased by the same pressure. In both cases, however, the relaxation time $\tau$ (or equivalently the relaxation frequency $f$) for the dielectric response and the dc conductivity $\sigma_{dc}$ change concomitantly, while the static dielectric constant is almost unchanged. To explain such temperature and pressure variations of both $\tau$ and $\sigma_{dc}$, we have suggested that they are both attributed to the variation of mobility $\mu$ of NI domain walls. The observed behaviors of the static dielectric constants, the relaxation time, and the dc conductivity as well, can be accounted for reasonably well by the kinetics of confined ionic domains and NI domain walls in the neutral $DA$ stacks. The interpretations developed in this paper are also consistent with the nonlinear dc transport phenomena recently found in TTF-CA by the present group.[13] The anomalous dielectric response also shows up as negative $\epsilon_1$ values at high pressures. This effect is attributed to the plasmonlike oscillation associated with the intermolecular charge-transfer instability.

Finally, we remark upon the following. The concept of solitonic and domain-wall-like nonlinear excitations in one-dimensional systems still remains hypothetical and hard to be proved directly by a single experiment. This is true in the case of mixed-valent organic crystals like TTF-CA, too. Nevertheless, to understand various experimental results of these organic materials as a whole, the concept of the collective excitations is becoming more and more important, not as a mere fashionable model, but as a useful model capable of predicting some hitherto unrevealed phenomena. In TTF-CA, the anomalous dielectric phenomena presently observed would not be foreseen to exist without the help of the concept of bound and mobile charged solitons and NI domain walls. This success has led us to the expectation that similar dielectric properties will be also observed in other mixed-stack $CT$ crystals as well, if they are located close to the NI phase boundary. Experimental results[30] have been found to be in good agreement with this prediction, as will be reported shortly, making us more confident of the model assumed in this paper.

## ACKNOWLEDGMENTS

We are grateful to Dr. N. Nagaosa for many enlightening discussions. The work done by the group of University of Tokyo (Y.T. and T.K.) was supported in part by a Grant for International Joint Research Project from the NEDO, Japan. Part of this work was supported by a Grant-in-Aid from the Ministry of Education, Science and Culture, Japan.

*Present address: Department of Chemistry, Kyoto University, Kyoto 606, Japan.

[1]J. B. Torrance, A. Girlando, J. J. Mayerle, J. I. Crowley, V. Y. Lee, P. Batail, and S. J. LaPlaca, Phys. Rev. Lett. **47**, 1747 (1981).

[2]J. B. Torrance, J. E. Vazquez, J. J. Mayerle, and V. Y. Lee, Phys. Rev. Lett. **46**, 253 (1981).

[3]Y. Tokura, Y. Kaneko, H. Okamoto, S. Tanuma, T. Koda, T. Mitani, and G. Saito, Mol. Cryst. Liq. Cryst. **125**, 71 (1985).

[4]A. Girlando, F. Marzola, C. Pecile, and J. B. Torrance, J.

Chem. Phys. **79**, 1075 (1983).
[5]S. Kagoshima, Y. Kanai, M. Tani, Y. Tokura, and T. Koda, Mol. Cryst. Liq. Cryst. **120**, 9 (1985).
[6]Y. Tokura, H. Okamoto, T. Koda, T. Mitani, and G. Saito, Solid State Commun. **57**, 607 (1986).
[7]M. Hanfland, A. Brillante, A. Girlando, and K. Syassen, Phys. Rev. B **38**, 1456 (1988).
[8]H. Okamoto, T. Koda, Y. Tokura, T. Mitani, and G. Saito, Phys. Rev. B **39**, 10 693 (1989).
[9]Y. Kaneko, S. Tanuma, Y. Tokura, T. Koda, T. Mitani, and G. Saito, Phys. Rev. B **35**, 8024 (1987).
[10]Y. Tokura, T. Koda, G. Saito, and T. Mitani, J. Phys. Soc. Jpn. **53**, 4445 (1984).
[11]T. Mitani, G. Saito, Y. Tokura, and T. Koda, Phys. Rev. Lett. **53**, 842 (1984).
[12]T. Mitani, Y. Kaneko, S. Tanuma, Y. Tokura, T. Koda, and G. Saito, Phys. Rev. B **35**, 427 (1987).
[13]Y. Tokura, H. Okamoto, T. Koda, T. Mitani, and G. Saito, Phys. Rev. B **38**, 2215 (1988).
[14]Y. Tokura, T. Koda, T. Mitani, and G. Saito, Solid State Commun. **43**, 757 (1982).
[15]C. S. Jacobsen and J. B. Torrance, J. Phys. Chem. **78**, 112 (1983).
[16]N. Nagaosa, Solid State Commun. **57**, 179 (1986).
[17]N. Nagaosa and J. Takimoto, J. Phys. Soc. Jpn. **55**, 2745 (1986).
[18]N. Nagaosa, J. Phys. Soc. Jpn. **55**, 2754 (1986).
[19]N. Nagaosa, J. Phys. Soc. Jpn. **55**, 3488 (1986).
[20]For reviews, see G. Grüner and A. Zettl, Phys. Rep. **119**, 117 (1985); A. A. Gogolin, *ibid.* **86**, 1 (1982).
[21]See, for example, H. Frohlich, *Theory of Dielectrics* (Clarendon Press, Oxford, 1958).
[22]Above about 4 kbar, the ac conductivities, that is, $\epsilon_1$ and $\epsilon_2$ could not be obtained exactly by the impedance analyzer (YHP 4194A) because of the large stray capacitance and reactance. By using the LCR meter (YHP 4274A) we obtained precisely the ac conductivities ($\epsilon_{1,2}$) at high pressures up to about 7 kbar. In this instrument (YHP 4274A), the ac conductivity measurements are possible only at the several fixed frequencies, as shown in Fig. 6.
[23]P. M. Lenahan and T. J. Rowland, Solid State Commun. **37**, 223 (1981).
[24]P. M. Lenahan and T. J. Rowland, Phys. Rev. B **23**, 752 (1981).
[25]In Fig. 2 only a part of data is plotted. Temperature dependence of $[\epsilon(0)-\epsilon_\infty]$ obtained from the results of Fig. 2 is slightly different from that of Fig. 1(a) as mentioned in Sec. III.
[26]G. Grüner, A. Zawadowski, and P. M. Chaikin, Phys. Rev. Lett. **46**, 511 (1981).
[27]Y. Tokura *et al.*, unpublished results.
[28]H. Okamoto *et al.*, unpublished results.
[29]R. M. Metzger and J. B. Torrance, J. Am. Chem. Soc. **107**, 117 (1985).
[30]Y. Tokura, S. Koshihara, Y. Iwasa, H. Okamoto, T. Komatsu, T. Koda, N. Iwasawa, and G. Saito, Phys. Rev. Lett. **63**, 2405 (1989).